

Quantification of quantum correlations in two-beam Gaussian states using photon-number measurements

Artur Barasiński^{a,b,*}, Jan Peřina Jr.^{a,†} and Antonín Černoch^c

^a*Joint Laboratory of Optics of Palacký University and Institute of Physics of CAS,
Faculty of Science, Palacký University, 17. listopadu 12, 771 46 Olomouc, Czech Republic*

^b*Institute of Theoretical Physics, University of Wrocław,
Plac Maxa Borna 9, 50-204 Wrocław, Poland and*

^c*Institute of Physics of the Czech Academy of Sciences,
Joint Laboratory of Optics of Palacký University and Institute of Physics of CAS,
17. listopadu 50a, 772 07 Olomouc, Czech Republic*

(Dated: September 13, 2022)

Identification and subsequent quantification of quantum correlations is critical for understanding, controlling and engineering quantum devices and processes. We derive and implement a general method to quantify various forms of quantum correlations using solely the experimental intensity moments up to the fourth order. This is possible as these moments allow for an exact determination of the global and marginal impurities of two-beam Gaussian fields. This leads to the determination of steering, tight lower and upper bounds for the negativity, and the Kullback-Leibler divergence used as a quantifier of state non-separability. The principal squeezing variances are determined as well using the intensity moments. The approach is demonstrated on the experimental twin beams with increasing intensity and the squeezed super-Gaussian beams composed of photon pairs. Our method is readily applicable to multi-beam Gaussian fields to characterize their quantum correlations.

Quantum theory allows for correlations between spatially separated systems or degrees of freedom that are fundamentally different from their classical counterparts. For composite systems, quantum correlations (QCs) manifest themselves in many different (inequivalent) forms [1–4], including the Bell nonlocality, quantum steering and entanglement. They can be exploited to achieve qualitatively better performance in information processing tasks compared to purely classical scenarios. Though the question of which kind of QCs is a necessary resource for a given quantum information protocol remains still open, particularly when multi-part systems are considered, the analysis of QCs among different subsystems is extraordinarily important [5, 6]. It belongs to fundamental problems in quantum information science and quantum many-body physics at present. Applying very general quantum theories and models, the structure of QCs is elucidated and non-trivial limitations on the strength of physically allowed QCs are revealed.

Over the years, several methods for the analysis of QCs have been proposed based on, e.g., the violation of various inequalities [7–10], geometrical considerations [11], or even interference among multiple copies of the investigated state [12–14]. However, such methods usually require certain initial knowledge about the analyzed state’s density matrix, which is never experimentally acquired without technical difficulties. Similarly, the homodyne tomography [15] in quantum optical experiments with continuous-variable states, which provides the complete characterization of the detected field, has to rely on a coherent local oscillator with the varying phase [16]. Contrary to this, we routinely measure the photocount distributions in numerous experiments by photon-number-resolving detectors [17]. So it is very important to de-

velop methods allowing to extract the maximum information about QCs in the analyzed field using just these photoncount distributions. While there are numerous non-classicality witnesses at our disposal [18–20], revealing the structure of QCs represents a much more complicated task. Several schemes for solving this problem have already been suggested using, however, some form of homodyning of the analyzed field [21–23]. Interestingly, an exact copy of the analyzed state can be used in a suitable interferometric setup [13] instead of a local coherent oscillator of the homodyne scheme to reveal all 4 invariants of a two-beam Gaussian field, which is equivalent to the determination of all elements of its covariance matrix.

In this Letter, we address this problem for a wide group of in-practise important Gaussian fields. We propose a scheme based solely on the intensity moments of optical fields to estimate their global and marginal purities. Although the photocount measurements do not allow for the determination of all coefficients characterizing such Gaussian fields (information about the phases of complex coefficients is missing), the needed information can partly be inferred from the values of higher-order intensity moments [24]. In our scheme, both the global and marginal field purities are expressed in terms of higher-order intensity moments. This opens the door for direct determination of important QC quantifiers, involving the Rényi-2 entropy, Kullback-Leibler divergence, one- and two-way Gaussian steering, and even tight lower and upper bounds for the logarithmic negativity. Also, the squeezing of Gaussian states can be determined. In practise, direct measurements of the intensity moments of optical fields are standardly performed using various types of photon-number-resolving detectors including intensified CCD cameras [25, 26]. This makes our scheme

qualitatively simpler compared to those based on various forms of homodyning. Using two-beam states originated in parametric down-conversion, we experimentally demonstrate the suggested approach.

Gaussian fields purity estimation.— We begin with defining the normal characteristic function $C_N(\beta_1, \beta_2)$ [24] for general two-beam fields,

$$C_N(\beta_1, \beta_2) = \langle \exp \left[\sum_{j=1,2} \beta_j \hat{a}_j^\dagger \right] \exp \left[- \sum_{j=1,2} \beta_j^* \hat{a}_j \right] \rangle, \quad (1)$$

where \hat{a}_j (\hat{a}_j^\dagger) stands for the annihilation (creation) operator of beam j , $j = 1, 2$ and $\langle \rangle$ denotes quantum-mechanical averaging. For quantum Gaussian fields the characteristic function $C_N(\beta_1, \beta_2)$ takes the form [24]:

$$C_N(\beta_1, \beta_2, \beta_1^*, \beta_2^*) = \exp \left[- \sum_{j=1,2} [B_j |\beta_j|^2 + (C_j \beta_j^{*2} / 2 + \text{c.c.})] + (D_{12} \beta_1^* \beta_2^* + \bar{D}_{12} \beta_1 \beta_2^* + \text{c.c.}) \right] \quad (2)$$

with real (B_j) and complex (C_j , D_{jk} , \bar{D}_{jk}) parameters characterizing the Gaussian state; c.c. replaces the complex-conjugated terms.

The measured intensity moments $\langle W_1^k W_2^l \rangle$, given as the normally-ordered photon-number moments and obtained via the Stirling numbers from the measured photon-number moments [24], contain partial information about the state parameters:

$$\langle W_1^k W_2^l \rangle = (-1)^{k+l} \frac{\partial^{2(k+l)} C_N(\beta_1, \beta_2, \beta_1^*, \beta_2^*)}{\partial^k \beta_1 \partial^k (\beta_1^*) \partial^l \beta_2 \partial^l (\beta_2^*)} \Big|_{\beta_1 = \dots = \beta_2^* = 0} \quad (3)$$

Considering the intensity moments up to the second order, we reveal the following relations for the looked-for parameters:

$$\begin{aligned} B_j &= \langle W_j \rangle, \\ |C_j|^2 &= \langle W_j^2 \rangle - 2\langle W_j \rangle^2, \quad j = 1, 2, \\ |D_{12}|^2 + |\bar{D}_{12}|^2 &= \langle W_1 W_2 \rangle - \langle W_1 \rangle \langle W_2 \rangle. \end{aligned} \quad (4)$$

The third-order intensity moments give us additional information about the looked-for parameters:

$$\begin{aligned} -4\Re\{C_1 \bar{D}_{12} D_{12}^*\} &= -4\langle W_1 \rangle (\langle W_1 W_2 \rangle - \langle W_1 \rangle \langle W_2 \rangle) \\ &\quad + \langle W_1^2 W_2 \rangle - \langle W_1^2 \rangle \langle W_2 \rangle, \\ -4\Re\{C_2^* \bar{D}_{12} D_{12}\} &= -4\langle W_2 \rangle (\langle W_1 W_2 \rangle - \langle W_1 \rangle \langle W_2 \rangle) \\ &\quad + \langle W_1 W_2^2 \rangle - \langle W_1 \rangle \langle W_2^2 \rangle. \end{aligned} \quad (5)$$

We note that, alternatively, the expressions in Eq. (5) can be obtained from the third-order moments $\langle W_j^3 \rangle$, $j = 1, 2$ or even fourth-order moments $\langle W_1^3 W_2 \rangle$ and $\langle W_1 W_2^3 \rangle$. Finally, also the fourth-order intensity moment $\langle W_1^2 W_2^2 \rangle$

reveals a useful relation among the looked-for parameters,

$$\begin{aligned} 4(2|D_{12}|^2 |\bar{D}_{12}|^2 + \Re\{C_1 C_2^* \bar{D}_{12}^2\} + \Re\{C_1 C_2 (D_{12}^*)^2\}) &= \langle W_1^2 W_2^2 \rangle - 4\langle W_1 W_2 \rangle^2 - \langle W_1 \rangle \langle W_2 \rangle \langle W_1 W_2 \rangle + \langle W_1 \rangle^2 \langle W_2 \rangle^2 \\ &\quad - 2[\langle W_1 \rangle^2 (\langle W_2^2 \rangle - 2\langle W_2 \rangle^2) + \langle W_2 \rangle^2 (\langle W_1^2 \rangle - 2\langle W_1 \rangle^2)] \\ &\quad - (\langle W_2^2 \rangle - 2\langle W_2 \rangle^2) (\langle W_1^2 \rangle - 2\langle W_1 \rangle^2) \\ &\quad + 16\langle W_2 \rangle \Re\{C_1 \bar{D}_{12} D_{12}^*\} + 16\langle W_1 \rangle \Re\{C_2^* \bar{D}_{12} D_{12}\}. \end{aligned} \quad (6)$$

Surprisingly, Eqs. (4)–(6) are sufficient to obtain the global and marginal purities of the two-beam Gaussian fields. In order to show that, we need to know the corresponding covariance matrix $\boldsymbol{\sigma} \equiv \langle \hat{\xi} \hat{\xi}^T \rangle - \langle \hat{\xi} \rangle \langle \hat{\xi}^T \rangle$ containing the second-order moments of the position $\hat{x}_j = (\hat{a}_j + \hat{a}_j^\dagger)/2$ and momentum $\hat{p}_j = (\hat{a}_j - \hat{a}_j^\dagger)/(2i)$ operators embedded in vector $\hat{\xi}^T = (\hat{x}_1, \hat{p}_1, \hat{x}_2, \hat{p}_2)$. Using the parameters of the normal characteristic function C_N in Eq. (2) the covariance matrix $\boldsymbol{\sigma}$ is expressed as:

$$\boldsymbol{\sigma} = \begin{bmatrix} \sigma_1 & \gamma \\ \gamma^T & \sigma_2 \end{bmatrix}, \quad (7)$$

where

$$\begin{aligned} \boldsymbol{\sigma}_j &= \begin{bmatrix} 1 + 2B_j + 2\Re\{C_j\} & 2\Im\{C_j\} \\ 2\Im\{C_j\} & 1 + 2B_j - 2\Re\{C_j\} \end{bmatrix}, \\ \boldsymbol{\gamma} &= \begin{bmatrix} 2\Re\{D_{12} - \bar{D}_{12}\} & 2\Im\{D_{12} - \bar{D}_{12}\} \\ 2\Im\{D_{12} + \bar{D}_{12}\} & -2\Re\{D_{12} + \bar{D}_{12}\} \end{bmatrix}. \end{aligned} \quad (8)$$

Now, one can easily verify that the determinants of the global $\boldsymbol{\sigma}$ and local $\boldsymbol{\sigma}_j$ covariance matrices are given in terms of the intensity moments as

$$\begin{aligned} \det \boldsymbol{\sigma} &= 1 + 4(\langle W_1 \rangle + \langle W_2 \rangle) + 12(\langle W_1 \rangle + \langle W_2 \rangle)^2 \\ &\quad - 4\langle W_1^2 \rangle (1 + 6\langle W_2 \rangle + 24\langle W_2 \rangle^2) - 4\langle W_2^2 \rangle \\ &\quad \times (1 + 6\langle W_1 \rangle + 24\langle W_1 \rangle^2) + 8\langle W_1^2 W_2 \rangle \\ &\quad \times (1 + 6\langle W_2 \rangle) + 8\langle W_1 W_2^2 \rangle (1 + 6\langle W_1 \rangle) \\ &\quad - 8\langle W_1 W_2 \rangle (1 + 6\langle W_1 \rangle + 6\langle W_2 \rangle + 48\langle W_1 \rangle \langle W_2 \rangle) \\ &\quad + 96\langle W_1 \rangle \langle W_2 \rangle (\langle W_1 \rangle + \langle W_2 \rangle + 5\langle W_1 \rangle \langle W_2 \rangle) \\ &\quad + 24\langle W_1^2 \rangle \langle W_2^2 \rangle - 8\langle W_1^2 W_2^2 \rangle + 48\langle W_1 W_2 \rangle^2, \end{aligned} \quad (9)$$

$$\det \boldsymbol{\sigma}_j = 1 + 4\langle W_j \rangle + 12\langle W_j \rangle^2 - 4\langle W_j^2 \rangle. \quad (10)$$

Knowing these determinants, the corresponding purities $\mu = 1/(\det \boldsymbol{\sigma})^{1/2}$ and $\mu_j = 1/(\det \boldsymbol{\sigma}_j)^{1/2}$ are established [1].

This central result allows us to determine various quantities that characterize the structure of two-beam QCs [27–30]. Using the purities μ and μ_j , $j = 1, 2$, we immediately obtain the Rényi-2 entropies along the formula $S_R = -\ln(\mu)$ [29]. We note that S_R represents the continuous analog of the Shannon entropy. The Rényi-2 entropy S_R can then be used to quantify the total quadrature correlations via the Kullback-Leibler divergence (distance) H between the analyzed two-beam state $\hat{\rho}$ and its factorized counterpart $\text{Tr}_2\{\hat{\rho}\} \text{Tr}_1\{\hat{\rho}\}$ [29]:

$$H = S_{R,1} + S_{R,2} - S_R = \ln \left(\frac{\mu}{\mu_1 \mu_2} \right). \quad (11)$$

Also the degree of (one-way) Gaussian steering of beam 2 by beam 1 [28] is expressed in terms of purities [30]:

$$G_{1 \rightarrow 2} = \max\{0, \ln(\mu/\mu_1)\}. \quad (12)$$

We note that two-way steering occurs provided that both $G_{1 \rightarrow 2}$ and $G_{2 \rightarrow 1}$ are nonzero.

Using purities, even the logarithmic negativity E_N [27], giving the degree of entanglement, is established through its tight lower and upper bounds derived by Adesso et al. [31]:

$$\begin{aligned} E_{\max}(\rho) &= -\frac{1}{2} \ln \left[-\frac{1}{\mu} + \left(\frac{\mu_1 + \mu_2}{2\mu_1^2\mu_2^2} \right) \right. \\ &\quad \left. \left(\mu_1 + \mu_2 - \sqrt{(\mu_1 + \mu_2)^2 - \frac{4\mu_1^2\mu_2^2}{\mu}} \right) \right], \\ E_{\min}(\rho) &= -\frac{1}{2} \ln \left[\frac{1}{\mu_1^2} + \frac{1}{\mu_2^2} - \frac{1}{2\mu^2} - \frac{1}{2} \right. \\ &\quad \left. - \sqrt{\left(\frac{1}{\mu_1^2} + \frac{1}{\mu_2^2} - \frac{1}{2\mu^2} - \frac{1}{2} \right)^2 - \frac{1}{\mu^2}} \right]. \quad (13) \end{aligned}$$

Application to experimental data.— We tested the derived formulas on a set of the experimental twin beams with increasing intensity [for mean photon number $\langle n_1 \rangle$ of beam 1, see Fig. 1(a)] that were obtained by adding the photocounts registered by two single-photon counting modules in the signal (1) and idler (2) beams in subsequent detection windows (for details, see [32]). We arrived this way at the compound twin beams with mean photon numbers extending over two orders in magnitude (from 0.1 to 10 mean photons per beam). The experimental photocount histograms were reconstructed by the maximum-likelihood approach to obtain the joint photon-number distribution $p(n_1, n_2)$ and its photon number moments $\langle n_1^k n_2^l \rangle_m = \sum_{n_1, n_2=0}^{\infty} n_1^k n_2^l p(n_1, n_2)$. Also entropy S of the fields was determined along the formula $S = -\sum_{n_1, n_2=0}^{\infty} p(n_1, n_2) \ln[p(n_1, n_2)]$ and plotted in Fig. 1(b). The intensity moments, that are the normally-ordered photon-number moments, were then derived as linear combinations of photon-number moments using the Stirling numbers of the first kind [18].

These experimental beams are multi-mode and suffer from imperfections that occur both during the generation process and transmission to the detectors. As a consequence, they decline from the theoretically expected form of a multi-mode noisy twin beam. These declinations can be quantified using the derived formulas for the tested quantum information quantities. However, they are derived for two single-mode beams and so their application is conditioned by the reduction of the experimental multi-mode photon-number moments $\langle n_1^k n_2^l \rangle_m$ to one typical mode. Estimating the number M of effective modes [20, 33] we may follow the procedure outlined in the Supplemental Material [34].

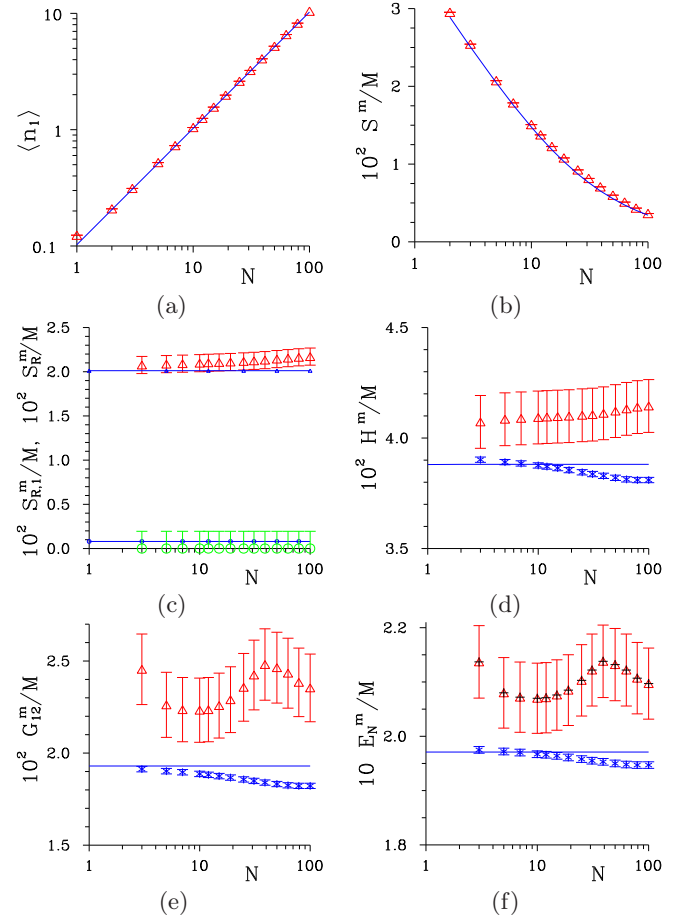


FIG. 1. (a) Mean photon number $\langle n_1 \rangle$ of beam 1 (red Δ), (b) entropy S^m/M per mode (red Δ), (c) Renyi-2 entropies per mode $S_{R,1}^m/M$ and S_R^m/M for beam 1 (red Δ) and beams 12 (green \circ), respectively, (d) Kullback-Leibler divergence per mode H^m/M and its value for noisy twin beam (blue $*$), (e) steering parameter per mode G_{12}^m/M (red Δ) and its value for noisy twin beam (blue $*$), and (f) lower (red Δ) and upper (black $+$) bounds for negativity per mode E_N^m/M and its value for noisy twin beam (blue $*$) as they depend on the number N of grouped detection windows; $M = 10N$ (for details, see [32]). In (a) and (b) error bars are smaller than the plotted symbols. In (f), red Δ and black $+$ nearly coincide. The solid blue curves originate in a model of M identical independent single-mode two-beam Gaussian fields with suitable parameters.

We compare the values of the obtained quantities per mode with those characterizing a single-mode Gaussian noisy twin beam, that is fully characterized by three first and second-order photon-number moments ($B_j = \langle w_j \rangle = \langle n_j \rangle$, $|D_{12}|^2 = \langle w_1 w_2 \rangle - \langle w_1 \rangle \langle w_2 \rangle = \langle n_1 n_2 \rangle - \langle n_1 \rangle \langle n_2 \rangle$). For the formulas, see the Supplemental Material [34].

According to the experimental results reduced to one mode and plotted in Figs. 1(c)–(f), the Renyi-2 entropies S_R^m/M , the Kullback-Leibler divergence H^m/M , the negativity E_N^m/M as well as the steering parameter $G_{1 \rightarrow 2}^m/M$ do not considerably change with the increasing

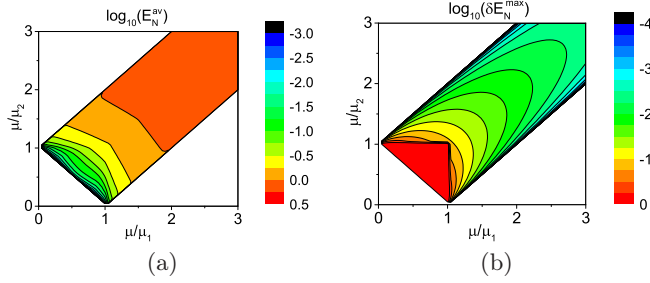


FIG. 2. (a) Average negativity E_N^{av} and (b) maximum δE_N^{max} of relative error as they depend on ratios μ/μ_1 and μ/μ_2 . In the white areas the states are not entangled. For $\mu_1 = \mu_2$, see also in [30].

field intensity, i.e. the increasing number N of grouped detection windows ($M = 10N$).

As the values of Renyi-2 entropy S_R^{m} of the two-beam fields are smaller than the entropies $S_{R,1}^{\text{m}}$ and $S_{R,2}^{\text{m}}$ of the constituting beams [see Fig. 1(c)], the purities of the two-beam fields are greater than those of the constituting beams. This implies, according to the general classification of two-beam Gaussian states (see Tab. 1 in [35]), that the analyzed two-beam fields are entangled.

The experimental values of the Kullback-Leibler divergence H_R^{m}/M , the one-way steering parameter $G_{1 \rightarrow 2}^{\text{m}}/M$ and the negativity E_N^{m}/M reduced per one mode and determined by the derived formulas (11)–(13) are systematically greater (by approximately 10% - 20%) than those characterizing the Gaussian noisy twin beams and determined by the formulas in the Supplemental Material. This means that the state of the detected two-beam fields is more general than that of the Gaussian noisy twin beams. The consideration of the experimental third- and fourth-order intensity moments reveals that also the complex parameters (C_j , $j = 1, 2$, and \bar{D}_{12}) of general two-beam Gaussian fields are nonzero, which leads, according to our results, to stronger QCs described by the above quantities.

The Kullback-Leibler divergence H_R^{m} , the steering parameter $G_{1 \rightarrow 2}^{\text{m}}$ and the negativity E_N^{m} of the two-beam fields increase practically linearly with the increasing twin-beam intensity. This contrasts with the behavior of the entropy S^{m} of the two-beam fields whose increase is smaller: The entropy S^{m}/M per mode plotted in Fig. 1(b) decreases with the increasing field intensity. This means that the capacity of available QCs increases linearly with the dimensionality (number of modes M) of the analyzed fields. The capacity of QCs thus grows faster than disorder in the analyzed fields quantified by the entropy S^{m} .

The negativity E_N is the most commonly used parameter to quantify QCs. However, we have only the lower and upper bounds in Eq. (13) at disposal for two-beam Gaussian fields. Nevertheless, the experimental data plotted in Fig. 1(f) show that these bounds are close to each

other, i.e. the uncertainty in determination of E_N is practically given only by the experimental errors. This observation is valid in general. Indeed, from the point of view of the entanglement, two-beam Gaussian states are divided into groups of states with identical amount of E_N . These groups are parameterized by 4 parameters: purities μ , μ_1 , μ_2 and serialian Δ [3]. The minimal and maximal values of the negativity E_N given in Eq. (13) in fact represent the extremal values with respect to serialian Δ for fixed values of the purities. The general behavior of these extremal values can conveniently be quantified taking into account that the negativity E_N increases (decreases) with the increasing global purity μ (marginal purities μ_1 and μ_2). This suggests the ratios μ/μ_j , $j = 1, 2$, as suitable parameters for quantifying the uncertainty in the determination of E_N : The greater the ratios are, the greater the negativity E_N is. This is documented in the graph of Fig. 2(a) where the negativity E_N^{av} averaged over the states with fixed ratios μ/μ_1 and μ/μ_2 is plotted. Maximum of the relative error δE_N^{max} [31],

$$\delta E_N = \frac{E_N^{\text{max}} - E_N^{\text{min}}}{E_N^{\text{max}} + E_N^{\text{min}}}, \quad (14)$$

taken over the states with the fixed ratios μ/μ_1 and μ/μ_2 is then shown in Fig. 2(b). According to Fig. 2(b), the relative error δE_N is smaller than 10% (1%) when the ratios μ/μ_j are greater than 1.5 (2.5), i.e. when the states exhibit considerable entanglement. This makes the use of the bounds for negativity E_N very efficient.

Single beam properties.— The above approach is useful also when nonclassical properties of individual beams are investigated. In this case, the intensity moments allow to determine the principal squeezing variance λ [36, 37],

$$\lambda = \min_{\varphi \in <0, 2\pi)} \langle [\Delta(\hat{a} \exp(i\varphi) + \hat{a}^\dagger \exp(-i\varphi))]^2 \rangle, \quad (15)$$

that quantifies the reduction of quantum noise below the shot-noise level, i.e. the level given by the Heisenberg uncertainty relations [17] ($\lambda < 1$). We have for a single-mode Gaussian field [24]

$$\lambda = 1 + 2(B - |C|) \quad (16)$$

using the coefficients in Eq. (3). The noise reduction may occur either in phase fluctuations or photon-number fluctuations. The reduction of phase fluctuations is found for degenerate parametric down-conversion that emits both photons from a pair into the same spatio-spectral mode. This results in very wide super-Gaussian statistics of photons in individual modes that is accompanied by the reduction of phase fluctuations below the shot-noise level [17]. When merging together the constituting beams of the above analyzed two-mode fields, i.e. when convolving their photon-number distributions, we arrive at the beam with such properties. Super-Gaussian character of

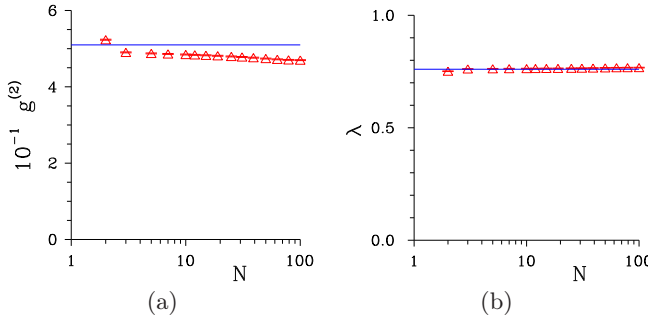


FIG. 3. (a) $g^{(2)}$ function and (b) principal squeezing variance λ of a beam obtained by merging the constituting beams of the analyzed two-beam fields as they depend on the number N of grouped detection windows. Experimental data are shown by red Δ with error bars smaller than the plotted symbols. The solid blue curves originate in a model of M identical independent single-mode two-beam Gaussian fields with suitable parameters.

the obtained beam, quantified by the values of $g^{(2)}$ function greater than 2, is demonstrated in Fig. 3(a). The corresponding values of the principal squeezing variance λ lower than 1 evidencing the generation of squeezed light are then shown in Fig. 3(b).

Further extension and application.— The obtained results can also be used to determine lower and/or upper bounds for other quantum information measures. For example, the Gaussian Rényi-2 entanglement measure $E_2(\rho_{12})$ is bounded by the relations $\frac{1}{2}H(\rho_{12}) \geq E_2(\rho_{12}) \geq G_{1 \rightarrow 2}(\rho_{12})$ [38]. Using the experimental data drawn in Figs. 1(d) and 1(e), the difference $\frac{1}{2}H(\rho_{12}) - G_{1 \rightarrow 2}(\rho_{12})$ has been found smaller than 10^{-4} for all analyzed two-beam fields, i.e. much smaller than the experimental errors.

Our results also allow for the analysis of QCs of general n -beam Gaussian states. This is so as the appropriate covariance matrix is composed of blocks of 2×2 matrices similar to those written in Eq. (7) [39, 40]. This allows to analyze its properties by considering all possible two-beam subsystems of the whole n -beam Gaussian field. The formulas in Eqs. (9) and (10) hold for such subsystems and allow to quantify QCs in these two-beam reductions. Relying on various monogamy relations, we may establish the lower bound for the genuine multipartite QCs in the whole n -beam field [29, 38, 41].

In conclusion, we have shown how various forms of quantum correlations of two-beam Gaussian fields (with multi-mode structure), that naturally depend on the fields phase properties, can be quantified solely from the measured intensity moments up to the fourth order. The determination of the global and marginal purities of the involved beams in terms of the intensity moments represents the key step. The principal squeezing variances can solely be derived from the intensity moments as well. We have demonstrated usefulness and practicality of this ap-

proach by considering suitable experimental fields. Our method is readily applicable to multipartite systems for the detection and characterization of their quantum correlations. As the Gaussian states are exploited in numerous metrology applications and quantum-information protocols with continuous variables, we foresee numerous applications of the suggested and demonstrated method in the near future.

A.B. acknowledges financial support by the Czech Science Foundation under the project No. 20-17765S. The authors thank the project CZ.02.1.01/0.0/0.0/16_019/0000754 of the Ministry of Education, Youth and Sports of the Czech Republic.

* artur.barasiński@uwr.edu.pl

† jan.perina.jr@upol.cz

- [1] Ch. Weedbrook, S. Pirandola, R. García-Patrón, N. J. Cerf, T. C. Ralph, J. H. Shapiro, and S. Lloyd, “Gaussian quantum information,” Rev. Mod. Phys. **84**, 621 (2012).
- [2] M. T. Quintino, T. Vértesi, D. Cavalcanti, R. Augusiak, M. Demianowicz, A. Acín, and N. Brunner, “Inequivalence of entanglement, steering, and bell nonlocality for general measurements,” Phys. Rev. A **92**, 032107 (2015).
- [3] G. Adesso, T. R. Bromley, and M. Cianciaruso, “Measures and applications of quantum correlations,” Journal of Physics A: Mathematical and Theoretical **49**, 473001 (2016).
- [4] G. De Chiara and A. Sanpera, “Genuine quantum correlations in quantum many-body systems: a review of recent progress,” Reports on Progress in Physics **81**, 074002 (2018).
- [5] A. Barasiński, A. Ćernoch, and K. Lemr, “Demonstration of controlled quantum teleportation for discrete variables on linear optical devices,” Phys. Rev. Lett. **122**, 170501 (2019).
- [6] A. Barasiński, I. I. Arkhipov, and J. Svozilík, “Localizable entanglement as a necessary resource of controlled quantum teleportation,” Sci. Rep. **8**, 15209 (2018).
- [7] Z.-B. Chen, J.-W. Pan, G. Hou, and Y.-D. Zhang, “Maximal violation of Bell’s inequalities for continuous variable systems,” Phys. Rev. Lett. **88**, 040406 (2002).
- [8] E. Shchukin and W. Vogel, “Inseparability criteria for continuous bipartite quantum states,” Phys. Rev. Lett. **95**, 230502 (2005).
- [9] A. Cavaillès, H. Le Jeannic, J. Raskop, G. Guccione, D. Markham, E. Diamanti, M. D. Shaw, V. B. Verma, S. W. Nam, and J. Laurat, “Demonstration of Einstein-Podolsky-Rosen steering using hybrid continuous- and discrete-variable entanglement of light,” Phys. Rev. Lett. **121**, 170403 (2018).
- [10] A. Barasiński, A. Ćernoch, W. Laskowski, K. Lemr, T. Vértesi, and J. Soubusta, “Experimentally friendly approach towards nonlocal correlations in multisetting N-partite Bell scenarios,” Quantum **5**, 430 (2021).
- [11] W. Laskowski, Ch. Schwemmer, D. Richart, L. Knips, T. Paterek, and H. Weinfurter, “Optimized state-independent entanglement detection based on a geometrical threshold criterion,” Phys. Rev. A **88**, 022327

- (2013).
- [12] P. Horodecki, "From limits of quantum operations to multicopy entanglement witnesses and state-spectrum estimation," *Phys. Rev. A* **68**, 052101 (2003).
- [13] J. Fiurášek and N. J. Cerf, "How to measure squeezing and entanglement of Gaussian states without homodyning," *Phys. Rev. Lett.* **93**, 063601 (2004).
- [14] K. Bartkiewicz, G. Chimczak, and K. Lemr, "Direct method for measuring and witnessing quantum entanglement of arbitrary two-qubit states through hong-ou-mandel interference," *Phys. Rev. A* **95**, 022331 (2017).
- [15] A. I. Lvovsky and M. G. Raymer, "Continuous-variable optical quantum-state tomography," *Rev. Mod. Phys.* **81**, 299 (2009).
- [16] O. Haderka, V. Michálek, V. Urbášek, and M. Ježek, "Fast time-domain balanced homodyne detection of light," *Appl. Opt.* **48**, 2884 (2009).
- [17] L. Mandel and E. Wolf, *Optical Coherence and Quantum Optics* (Cambridge Univ. Press, Cambridge, 1995).
- [18] J. Peřina Jr., I. I. Arkhipov, V. Michálek, and O. Haderka, "Non-classicality and entanglement criteria for bipartite optical fields characterized by quadratic detectors," *Phys. Rev. A* **96**, 043845 (2017).
- [19] J. Peřina Jr., O. Haderka, and V. Michálek, "Non-classicality and entanglement criteria for bipartite optical fields characterized by quadratic detectors II: Criteria based on probabilities," *Phys. Rev. A* **102**, 043713 (2020).
- [20] J. Peřina Jr., P. Pavlíček, V. Michálek, R. Machulka, and O. Haderka, "Nonclassicality criteria for n-dimensional optical fields detected by quadratic detectors," *Phys. Rev. A* **105**, 013706 (2022).
- [21] I. I. Arkhipov and J. Peřina Jr., "Retrieving the covariance matrix of an unknown two-mode Gaussian state by means of a reference twin beam," *Opt. Commun.* **375**, 29–33 (2016).
- [22] B. Kuhn, W. Vogel, and J. Sperling, "Displaced photon-number entanglement tests," *Phys. Rev. A* **96**, 032306 (2017).
- [23] I. I. Arkhipov, "Complete identification of nonclassicality of Gaussian states via intensity moments," *Phys. Rev. A* **98**, 021803(R) (2018).
- [24] J. Peřina, *Quantum Statistics of Linear and Nonlinear Optical Phenomena* (Kluwer, Dordrecht, 1991).
- [25] O. Haderka, J. Peřina Jr., M. Hamar, and J. Peřina, "Direct measurement and reconstruction of nonclassical features of twin beams generated in spontaneous parametric down-conversion," *Phys. Rev. A* **71**, 033815 (2005).
- [26] R. Machulka, O. Haderka, J. Peřina Jr., M. Lamperti, A. Allevi, and M. Bondani, "Spatial properties of twin-beam correlations at low- to high-intensity transition," *Opt. Express* **22**, 13374 (2014).
- [27] S. Hill and W. K. Wootters, "Computable entanglement," *Phys. Rev. Lett.* **78**, 5022 (1997).
- [28] E. G. Cavalcanti, S. J. Jones, H. M. Wiseman, and M. D. Reid, "Experimental criteria for steering and the Einstein-Podolsky-Rosen paradox," *Phys. Rev. A* **80**, 032112 (2009).
- [29] G. Adesso, D. Girolami, and A. Serafini, "Measuring gaussian quantum information and correlations using the rényi entropy of order 2," *Phys. Rev. Lett.* **109**, 190502 (2012).
- [30] I. Kogias, A. R. Lee, S. Ragy, and G. Adesso, "Quantification of Gaussian quantum steering," *Phys. Rev. Lett.* **114**, 060403 (2015).
- [31] G. Adesso, A. Serafini, and F. Illuminati, "Determination of continuous variable entanglement by purity measurements," *Phys. Rev. Lett.* **92**, 087901 (2004).
- [32] J. Peřina Jr., A. Černoch, and J. Soubusta, "Compound twin beams without the need of genuine photon-number-resolving detection," *Phys. Rev. Applied* **16**, 024061 (2021).
- [33] V. Michálek, J. Peřina Jr., and O. Haderka, "Experimental quantification of the entanglement of noisy twin beams," *Phys. Rev. Applied* **14**, 024003 (2020).
- [34] A. Barasiński, J. Peřina Jr., and A. Černoch, "Supplemental material," .
- [35] G. Adesso, A. Serafini, and F. Illuminati, "Extremal entanglement and mixedness in continuous variable systems," *Phys. Rev. A* **70**, 022318 (2004).
- [36] A. Lukš, V. Peřinová, and J. Peřina, "Principal squeezing of vacuum fluctuations," *Opt. Commun.* **67**, 149–151 (1988).
- [37] V. V. Dodonov, "Nonclassical states in quantum optics: A squeezed review of the first 75 years," *J. Opt. B: Quantum Semiclass. Opt.* **4**, R1–R33 (2002).
- [38] L. Lami, Ch. Hirche, G. Adesso, and A. Winter, "Schur complement inequalities for covariance matrices and monogamy of quantum correlations," *Phys. Rev. Lett.* **117**, 220502 (2016).
- [39] G. Adesso, A. Serafini, and F. Illuminati, "Quantification and scaling of multipartite entanglement in continuous variable systems," *Phys. Rev. Lett.* **93**, 220504 (2004).
- [40] G. Adesso, A. Serafini, and F. Illuminati, "Multipartite entanglement in three-mode Gaussian states of continuous-variable systems: Quantification, sharing structure, and decoherence," *Phys. Rev. A* **73**, 032345 (2006).
- [41] Y. Xiang, I. Kogias, G. Adesso, and Q. He, "Multipartite Gaussian steering: Monogamy constraints and quantum cryptography applications," *Phys. Rev. A* **95**, 010101(R) (2017).